Food Hydrocolloids 135 (2023) 108174

Contents lists available at ScienceDirect

Food Hydrocolloids

journal homepage: www.elsevier.com/locate/foodhyd

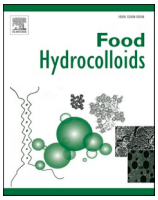

Ultrasound-treatment as a promising strategy to develop biodegradable films obtained from mushroom waste biomass

Zaida Pérez-Bassart [a,b], Antonio Martínez-Abad [a,b], Alcira Reyes [a,b], Amparo López-Rubio [a,b], María José Fabra [a,b,*]

[a] Food Safety and Preservation Department, Institute of Agrochemistry and Food Technology (IATA-CSIC), Valencia, Spain
[b] Interdisciplinary Platform for Sustainable Plastics Towards a Circular Economy- Spanish National Research Council (SusPlast-CSIC), Madrid, Spain

ARTICLE INFO

Keywords:
Valorisation
Biomass
Biopolymers
Packaging
Fungi

ABSTRACT

This work reports on the valorisation of discarded mushroom biomass generated in the industry and the waste produced after a β-glucan extraction process from three different species (*Grifola frondosa, Lentinula edodes,* and *Pleurotus ostreatus*) for the production of biobased and biodegradable films. Initially, the composition of the starting material was characterized before film production. The results evidenced no significant compositional differences between the discarded mushrooms, proteins, and β-glucans being the main components in all varieties. In contrast, the residues were mainly composed of carbohydrates (glucans and chitin).

The films obtained from the residues presented a very rigid behaviour, with higher elastic modulus (ca. 2–4.5 GPa) and lower elongation values (ca. 1%) compared to their counterparts prepared with the mushroom's discards. The developed films outperformed benchmark biopolymers in terms of barrier properties with the additional advantages that they can be directly produced from fungal biomass (without plasticizers or any other additives) and they proved to be easily disintegrated according to the standard ISO 20200.

1. Introduction

The global mushroom cultivation market is considerably growing and is expected to reach $52 billion by 2026, posing an environmental challenge for the main industries that market these products worldwide (Fortune Business Insights, 2019). Mushroom waste is mainly composed of mushrooms with misshapen caps and/or stalks that do not meet the specifications set by retailers but have high nutritional value (Aguiló-Aguayo, Walton, Viñas, & Tiwari, 2017). Therefore, researchers are looking for ways to turn the significant amount of waste produced from mushroom cultivation into valuable products since they offer significant economic potential as fungal cell walls contain chitin, hemicelluloses, and, among the most interesting functional components, β-glucans (Muzzarelli et al., 2012; Synytsya & Novák, 2013). Their valorisation has been gaining attention not only because of the health-promoting effects of β-glucans but also due to the different potential industrial applications, their impact on the economy, and the support for sustainability. Several valorisation schemes have been proposed from mushroom' waste and by-products to obtain valuable compounds (Grimm & Wösten, 2018; Zhu, Du, & Xu, 2016). Of especial interest is the integrated value chains as one of the most promising pathways to achieve the zero-waste goal and to accelerate the transition of the mushroom industry to a circular bioeconomy. For instance, the use of the waste streams, generated after β-glucans extraction from mushrooms' residues and by-products, to develop biopolymers is an underexplored area but with a great potential since some of the components present in the native mushrooms (i.e. chitin and recalcitrant β-glucans), remain in the residue (Ifuku, Nomura, Morimoto, & Saimoto, 2011).

Over the last decades, plastics have been widely used with an alarmingly growing rate of global production (Payne, McKeown, & Jones, 2019), raising concerns related to their waste management and environmental contamination, thus urging to look for alternatives. In this context, it is worth mentioning the current open debate and activity around plastic packaging and its environmental impacts that have mainly focused on the grocery and food retail sectors. Packaging has become an essential element in the commercialization of food products, being fundamental to ensuring food quality and safety and facilitating purchasing and transportation activities throughout "the farm to fork chain", contributing to reducing food waste (Bhargava, Sharanagat,

* Corresponding author. Food Safety and Preservation Department, Institute of Agrochemistry and Food Technology (IATA-CSIC), Valencia, Spain.
E-mail address: mjfabra@iata.csic.es (M.J. Fabra).

https://doi.org/10.1016/j.foodhyd.2022.108174
Received 4 July 2022; Received in revised form 30 August 2022; Accepted 17 September 2022
Available online 24 September 2022

Mor, & Kumar, 2020). Food packaging is a challenging part of the global plastics waste management challenge, representing the most significant demand for plastic packaging (Europe, 2021). Therefore, replacing synthetic plastics by biodegradable polymers from renewable natural resources (i.e. biopolymers) is envisaged as the most sustainable and long-term solution (George, Sanjay, Srisuk, Parameswaranpillai, & Siengchin, 2020; Savadekar & Mhaske, 2012). There is an increasing research interest in developing environmentally and economically sustainable packaging materials using more environmentally friendly alternatives that follow the Circular Economy principles (European Bioplastics, www.european-bioplastics.org). However, biopolymers' physicochemical properties (mechanical and barrier performance) are not comparable to benchmark synthetic polymers, and their production costs are too high to compete in the market. Most of these biopolymers need the addition of plasticizers, nucleating agents, or further additives to reach desirable mechanical properties, which pose disadvantages in their barrier properties, compostability, and even ecoxitological effects. Furthermore, the raw materials normally used for the production of biopolymers come from land crops, whose primary use is the food and feed sectors. As an alternative, agrifood waste and by-products are also being explored as a source for biopolymer production.

This work is focused on the valorisation of discarded mushroom biomass generated in the industry and the waste produced after β-glucan extraction from three different species (*Grifola frondosa, Lentinula edodes* and *Pleurotus ostreatus*) for the production of biopolymeric films. The suitability of both the discarded mushrooms (rejected biomass) and the residues to produce biopolymeric films was evaluated, investigating the effect of their composition on the performance of the biopolymeric films for their use as food packaging materials.

2. Methods and materials

2.1. Raw materials

The three fungal species (*Grifola frondosa, Lentinula edodes* and *Pleurotus ostreatus*) were kindly donated by Centro Tecnológico de Investigación del Champiñón –Asochamp- (Rioja, Spain). The extraction of β-glucans was carried out by means of using hot water treatments followed by an alkali treatment with NaOH, as described in previous work (Pérez-Bassart, Fabra, Martínez-Abad, & López-Rubio, 2023) with some modifications. Briefly, 25 g of freeze-dried raw material were subjected to an aqueous treatment at 100 °C with reflux with 300 mL of distilled water, stirring for 7 h. The resulting soluble part was concentrated and lyophilised. The precipitate obtained from centrifugation was subjected to an alkaline treatment at room temperature overnight with 300 mL of 1 M NaOH and 0.05% $NaBH_4$ to prevent peeling at the reducing end of the polysaccharides. The suspension obtained was then centrifuged. The supernatant was reserved for precipitation with 1:3 (v/v) ethanol to remove low molecular weight components and then dialysed and lyophilised to remove traces of NaOH. The remaining precipitate was washed with distilled water until neutral pH to ensure that the remaining NaOH was removed. This insoluble residue was referred to as fraction R, with GR, LR or PR, depending on the species, and was used for film development.

2.2. Chemical analysis of the raw material and waste fungal biomass

The protein content in whole mushrooms was calculated based on the nitrogen content estimated with the Kjeldahl method, multiplied by a factor 4.38 (Kalač, 2009). The protein content was calculated in both the whole mushroom and the residue by difference from the total elemental nitrogen and subtracting the nitrogen from D-glucosamine from the chitin, as previously described in Pérez-Bassart, Fabra, Martínez-Abad, & López-Rubio, 2023. The lipid content was estimated after performing the Soxhlet extraction according to AOAC method 933.06 with slight modifications. Approximately 5 g of raw material was extracted using Soxhlet apparatus with 250 mL of hexane over 8 h. The ash content was determined using the standard method TAPPI T211.

The monosaccharide composition, including the chitin content, from the discarded biomass and the residues, was determined as previously described in Pérez-Bassart, Fabra, Martínez-Abad, & López-Rubio, 2023. All experiments were carried out in triplicate.

2.3. Production of fungal-based films

Fungal-based films were produced by adding 1.5 g of the discarded biomass, or the residue generated after the β-glucan extraction protocol, to 100 mL of distilled water. The solution was dispersed using an ultra-turrax homogenizer (D9, MICCRA GmbH, Müllheim, Deutschland) (UT) at 20000 rpm for 1 min or sonication (US) using an UP-400S ultrasound equipment (Hielcher GmbH, Germany) at 400 W for 1 min. These were then evenly spread over a Teflon casting plate resting on a leveled surface. Films were formed by drying for 48 h at 56% RH at 25 °C. These conditions were selected after previous experiments to guarantee that homogeneous dry films could be peeled intact from the casting plate. The formed films were peeled off the casting plate and preconditioned at 53% RH for one week in a cabinet using magnesium nitrate oversaturated solution before analysis.

2.4. Scanning electron microscopy (SEM)

SEM was conducted on a Hitachi microscope (Hitachi S-4800) at an accelerating voltage of 10 kV and a working distance of 8–12 mm. Two different samples of each film were cryo-fractured after immersion in liquid nitrogen and randomly broken to investigate the cross-section of the samples. Samples were fixed on M4 Aluminium Specimen Mount and sputtered with a gold-palladium mixture under vacuum before their morphology was examined.

2.5. Optical properties

The transparency of the films was determined through the surface reflectance spectra in a spectrophotometer CM-26D (Minolta Co., Tokyo, Japan) with a 10 mm illuminated sample area. Measurements were taken from three samples in each film using both a white and a black background. The transparency was determined by applying the Kubelka–Munk theory for multiple scattering to the reflection spectra. Transparency (Ti) (0–100 theoretical range) was calculated from the reflectance of the sample layer on a white background of known reflectance and on an ideal black background, as described in (Fabra, Talens, & Chiralt, 2009).

2.6. Fourier transform infrared spectroscopy (FT-IR)

Film samples were analyzed by FT-IR in attenuated total reflectance (ATR) mode using a Thermo Nicolet Nexus (GMI, USA) equipment. The spectra were taken at 4 cm^{-1} resolution in a wavelength range between 400 and 4000 $^{-1}$ and averaged a minimum of 32 scans. The results were processed using Origin Pro 2019 software.

2.7. X-ray diffraction (XRD)

XRD measurements of the films were carried out at room temperature on a D5005 Bruker diffractometer. The instrument was equipped with a Cu tube and a secondary monochromator. The configuration of the equipment was θ–2θ, and the samples were examined over the angular range between 3° and 60° with a step size of 0.02° and a count time of 200 s per step.

2.8. Thermal properties

Thermogravimetric curves (TG) of the discarded biomass and the

residues were recorded with a TA 550 (Waters- TA Instruments, New Castle, EEUU). The samples (*ca.* 5 mg) were heated from 30 to 700 °C with a heating rate of 10 °C/min under a nitrogen atmosphere. Derivative TG curves (DTG) expressed the weight loss rate as a function of temperature and were plotted using Origin Pro 2019 software.

Thermal properties of the films were also evaluated by Differential Scanning Calorimetry (DSC) using a TA Instrument (New Castle, DE, USA) thermal analysis system under nitrogen atmosphere. The analysis was carried out oñ3 mg of each sample at a heating rate of 10 °C/min, from 20 °C to 450 °C. The DSC equipment was calibrated with indium as a standard and the slope of the thermograms was corrected by subtracting similar scans of an empty pan. Tests were done in triplicate.

2.9. Water vapor permeability (WVP)

Direct permeability to water vapor was determined from the slope of the weight gain versus time curves at 23 °C, using the ASTM 2010 gravimetric method. Tests were done in triplicate for each sample type, and water vapor permeability was carried out at 0–75% relative humidity gradient. The films were sandwiched between the aluminium top (open O-ring) and bottom (deposit for silica gel) parts of Payne permeability cups (3.5 cm diameter, Elcometer SPRL, Hermelle/s Argenteau, Belgium). A Viton rubber O-ring was placed between the film and bottom part of the cell to enhance sealability. Permeability cups containing silica were placed in an equilibrated cabinet at 75% RH using an oversaturated sodium chloride salt solution.

2.10. Oxygen permeability (OP)

Oxygen permeability (OP) was calculated from oxygen transmission rate (OTR) measurements recorded in triplicate using an Oxygen Permeation Analyzer 8001 (Systech Illinois, UK). The samples were previously purged with nitrogen in the humidity equilibrated test cell, before exposure to an oxygen flow of 10 mL min^{-1}. The exposure area during the test was 5 cm^2 for each sample. In order to obtain the oxygen permeability, film thickness and gas partial pressure were considered in each case. Experiments were carried out at 23 (±1) °C and 53 (±2) % RH.

2.11. Mechanical properties

A universal test Machine (Instron, USA) was used to determine the tensile strength (TS), elastic modulus (E), and elongation at break (ϵ_b) of the films, according to ASTM standard method D882.10 (ASTM, 2001). Tensile parameters were determined from the stress-strain curves, estimated from force-distance data obtained for the different films (1 cm wide and 8 cm long). At least eight replicates were obtained per formulation. Pre-conditioned specimens were mounted in the film-extension grips of the testing machine and stretched at 50 mm min^{-1} until breaking. The relative humidity of the environment was held constant at 54 (±2) % during the tests, which were performed at 23 (±1) °C.

2.12. Water contact angle measurements

The surface hydrophobicity as the wettability of fungal-based films were measured in a DSA25 equipment (Kruss) equipped with image analysis AD4021 software at ambient conditions. A precision syringe deposited a water droplet (~3 μL) on the film surface. Contact angle values were obtained by analyzing the shape of the distilled water drop after it had been placed over the film for 10s. Five replicates were analyzed per film formulation.

2.13. Water uptake

The water absorption behavior of the films was determined. The samples were dried prior to testing at 60 °C to constant weight. They were then placed in a 75% RH equilibrated cabinet with a supersaturated sodium chloride salt solution and gravimetric measurements were performed until constant weight. For each type of sample, the tests were carried out in triplicate. The water absorption content was calculated as a percentage of weight gained concerning the initial weight of the sample.

2.14. Disintegration tests

The disintegration test of the mushroom-derived films was carried out following several guidelines of the standard ISO 20200:2016. In this test, a synthetic solid consisting of a mixture of sawdust, rabbit feed, mature compost, corn starch, sucrose, corn oil, urea and water is used to simulate laboratory scale composting conditions and the samples to be tested are composted with this prepared solid matrix.

One test reactor (consisting of a polypropylene container) per sample was prepared and each reactor contained 5 g of film and 1 kg of wet synthetic solid. The mass ratio of the films vs. the wet synthetic residue was between 0.5% and 2.0%, according to the standard method.

The reactors were incubated at a temperature of 58 ± 2 °C for a minimum of 45 days. The contents of the reactors were regularly mixed and moistened (final water content of 55% in total) to guarantee an excellent composting process. During the composting period, the gross mass of the composting container was totally or partially restored according to the schedule established in the calendar indicated by the standard method.

The degree of disintegration was determined after the composting period by sieving the final matrix through standard 10 mm, 5 mm, and 2 mm sieves (according to ISO 3310–1) to recover the non-disintegrated material. The mass reduction of the tested films was considered as disintegrated material and was used to calculate the degree of disintegration.

2.15. Statistical analysis

Statistical analysis of results was carried out with Statgraphics using one-way analysis of variance (ANOVA) to determine the significant differences between samples, at a significance level of $P < 0.05$.

3. Results and discussion

3.1. Compositional characterization of the mushrooms' discards and the residue

In the first stage of this work, the composition of the three different mushrooms (*Grifola frondosa, Lentinula edodes, and Pleurotus ostreatus*) and the residue generated after β-glucan extraction (applying hot-water treatments followed by alkali treatments) was characterized before film production. The results, shown in Table 1, evidenced no significant compositional differences between the discarded mushrooms, except for the higher lipid content of *Grifola frondosa* and *Lentinula edodes* compared to *Pleurotus ostreatus*. This agrees with a previous work in which very similar composition was reported for the three different mushroom varieties (Pérez-Bassart, Fabra, Martínez-Abad, & López-Rubio, 2023). As expected, proteins and β-glucans represented all varieties' main components, with *ca.* 22, 23 and 24% protein contents for *L. edodes, G. frondosa* and *P. ostreatus*, respectively. As observed in Fig. 1, *P. ostreatus* had the most meaningful β-glucan content (*ca.* 43%), higher than that of the other two mushroom species (*ca.* 36 and 31% for *G. frondosa* and *L. edodes*, respectively). Chitin content was lower in *L. edodes* than in the other two species, within the range reported for wild mushroom species (2–8.5% of the dry matter) (Vetter, 2007). Additionally, the polyphenol content (expressed as mg of gallic acid –GA- per gram of sample) of the discarded biomass was higher for *G. frondosa.* It should be noted that although a lower polyphenol content

Table 1
Proximal composition and antioxidant capacity of the discarded biomass and the residue.

Sample *	Protein (%)	Lipids (%)	Carbohydrates (%)	Ashes (%)	Polyphenols (mgGA/gDW)**	TEAC (μg TE/g DW)***
G	23.55 (0.25) ^{ab}	8.23 (0.23) ^{a}	50.87 (1.67) ^{a}	5.95 (0.01) ^{a}	92.03 (6.83) ^{a}	150.59 (5.30) ^{a}
GR	6.59 (0.10) ^{c}	<0.1	92.05 (5.19) ^{d}	1.13 (0.37) ^{c}	7.33 (0.13) ^{c}	16.28 (1.29) ^{c}
L	22.21 (0.18) ^{a}	7.22 (0.30) ^{b}	41.91 (4.08) ^{a}	6.54 (0.30) ^{a}	58.93 (2.92) ^{b}	124.67 (5.60) ^{b}
LR	6.63 (0.03) ^{c}	<0.1	69.65 (1.09) ^{bc}	1.03 (0.21) ^{c}	7.42 (0.21) ^{c}	10.89 (0.89) ^{d}
P	24.05 (1.09) ^{b}	5.35 (0.39) ^{c}	51.81 (3.82) ^{ab}	7.82 (0.01) ^{b}	61.51 (1.25) ^{b}	149.20 (4.36) ^{a}
PR	7.52 (0.00) ^{c}	<0.1	78.71 (5.03) ^{c}	1.30 (0.35) ^{c}	7.14 (0.04) ^{c}	15.08 (2.34) ^{cd}

Mean values (standard deviation). Values with different letters in the same column are significantly different ($p \leq 0.05$). *G: *G. frondosa* whole mushroom; L: *L edodes* whole mushroom; P: *P. ostreatus* whole mushroom; GR: residue from *G. frondosa* left after the aqueous and alkaline treatments, LR: residue from *L. edodes* left after the aqueous and alkaline treatments PR: residue from *P.ostreatus* left after the aqueous and alkaline treatments **mg of gallic acid equivalents per 100 g of dry weight (DW). ***μg Trolox Equivalent per gram of DW. *** Concentration that inhibits 50% of discoloration of β-carotene. DW: dry weight.

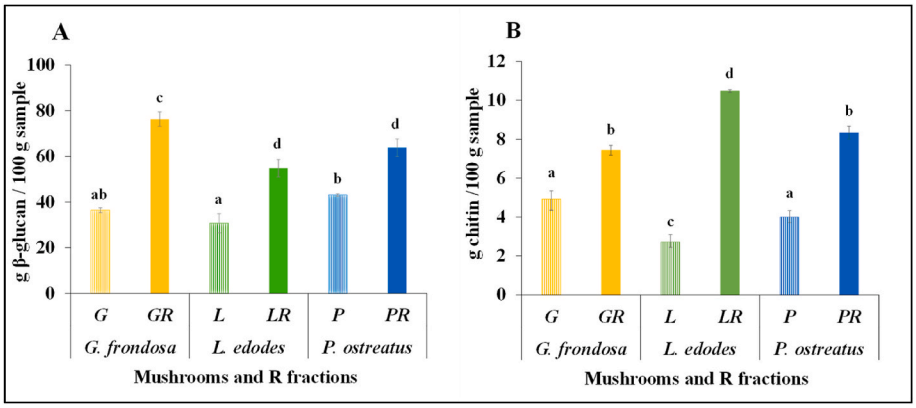

Fig. 1. **(A)** β-glucan and **(B)** chitin content of the mushrooms' discards and residues. Values followed by different letters are significantly different ($p \leq 0.05$).

was found in discarded *P. ostreatus* biomass, no significant differences were observed in the antioxidant activity when *G. frondosa* and *P. ostreatus* were compared. This effect indicates that the antioxidant activity of *P. ostreatus* was not only given by the phenolic compounds but other molecules, such as *β*-glucans with reported antioxidant properties could have also contributed to the observed TEAC values.

The composition of the residues obtained after subjecting the fungal biomass to the β-glucan extraction protocols previously described is also shown in Table 1. The residual yields were 19.28 ± 0.97, 23.36 ± 0.47, and 22.54 ± 0.59% for *G. frondosa, L. edodes,* and *P. ostreatus*, respectively. Not surprisingly, the residues contained a significant amount of chitin and minor amounts of protein. Chitin was more abundant in the *L. edodes* residue than in the other two residues. A significant amount of β-glucan remained in the residues even after aqueous and alkaline extraction. Between the three species, it was significantly higher for *G. frondosa*, thus confirming its excellent recalcitrance nature, probably ascribed to stronger β-glucan-chitin bonds (as it did not have higher chitin content). Compared to the discarded biomass, the higher amount of glucans in the residue indicated that they were concentrated, even after soluble β-glucan extraction since other more soluble components (such as proteins, ashes and polyphenols) were more efficiently removed during the aqueous and alkaline treatments. Although the internal structure and molecular weight of the β-glucans in the residues may substantially differ between species, significant differences in total β-glucan were only observed between *G. frondosa* and the other two species. Although in minor amounts (<8%), heteropolysaccharides such as xylomannans, mannogalactans, fucomannogalactans or xyloglucans (see Fig. S1 for detailed composition) might have also influenced the film's thermo-mechanical properties. Furthermore, the antioxidant activity and the phenolic compounds of the residues were significantly reduced compared to the discarded mushroom biomass.

Additionally, TGA characterization was carried out to determine the thermal stability of the discarded biomass and the residues, and the results are shown in Fig. 2. As deduced from the derivative thermogravimetric profiles, all species from the discarded mushroom biomass degraded at lower temperatures than the residue. Discarded mushrooms showed very similar behavior, typical of multicomponent materials, with an initial degradation shoulder between 135 and 175 °C ascribed to

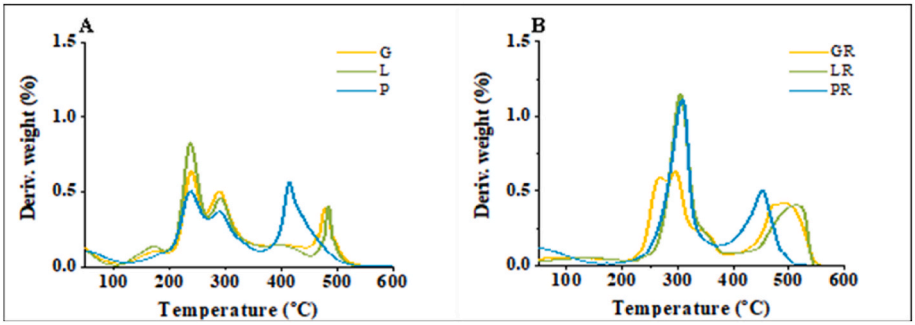

Fig. 2. Derivative thermogravimetric (DTG) curves of the **(A)** mushrooms' discards and **(B)** the residue.

the tightly bound water and the degradation of low molecular weight compounds present in the mushrooms' cell walls. A broad degradation profile, around 230 to 300 °C, was ascribed to the contribution of both β-glucans and chitin (Aburas, İspirli, Taylan, Yilmaz, & Dertli, 2020; Eyigor, Bahadori, Yenigun, & Eroglu, 2018; Puanglek et al., 2016), in agreement to that found for commercial glucans and chitin samples (see Fig. S2 from Supplementary Material). The last degradation sharp peak with a maximum at 413 °C for *P. ostreatus* and 484 °C for *G. frondosa* and *L. edodes* is related to the degradation of chitin-glucan complexes and pure chitin (Girometta et al., 2020). Analogous to these findings, the DTG curve of the chitin standard reports a peak at around these temperatures (see Fig. S2 from Supplementary Material). The different behavior found in the last degradation peak supports the presence of β-glucan-chitin complexes in *G. frondosa* and the less recalcitrant nature of β-glucans from *P. ostreatus*, which clearly showed the degradation peak of chitin centered at 413 °C.

When compared with the residues, the first thing to highlight is that the maxima of the degradation peaks appeared at temperatures higher than the discarded biomass, indicating the higher thermal stability of the residues. It should be noted that *P. ostreatus* and *L. edodes* residues showed a thermal degradation profile characterized by an initial sharp peak in the temperature range of 305 and 351 °C, which can be ascribed to the degradation of β-glucans and chitin. The same degradation peak, although with broader distribution, was observed for *G. frondosa*, showing a similar degradation profile to its counterpart discarded biomass and confirming the presence of more recalcitrant β-glucans from the *G. frondosa* residue, which are still linked to the chitin in the residues. The last degradation peak observed in all the residues, mainly ascribed to the contribution of the chitin and glucan-chitin complexes, showed a broader distribution in the *L. edodes* and *G. frondosa* residues than in their counterparts' discarded biomass, being more accentuated in *G. frondosa*.

3.2. Characterization of mushroom films from the mushrooms' discards and the residue

The discarded mushroom biomass was used to generate films from aqueous suspensions using UT and US treatments. It is interesting to note

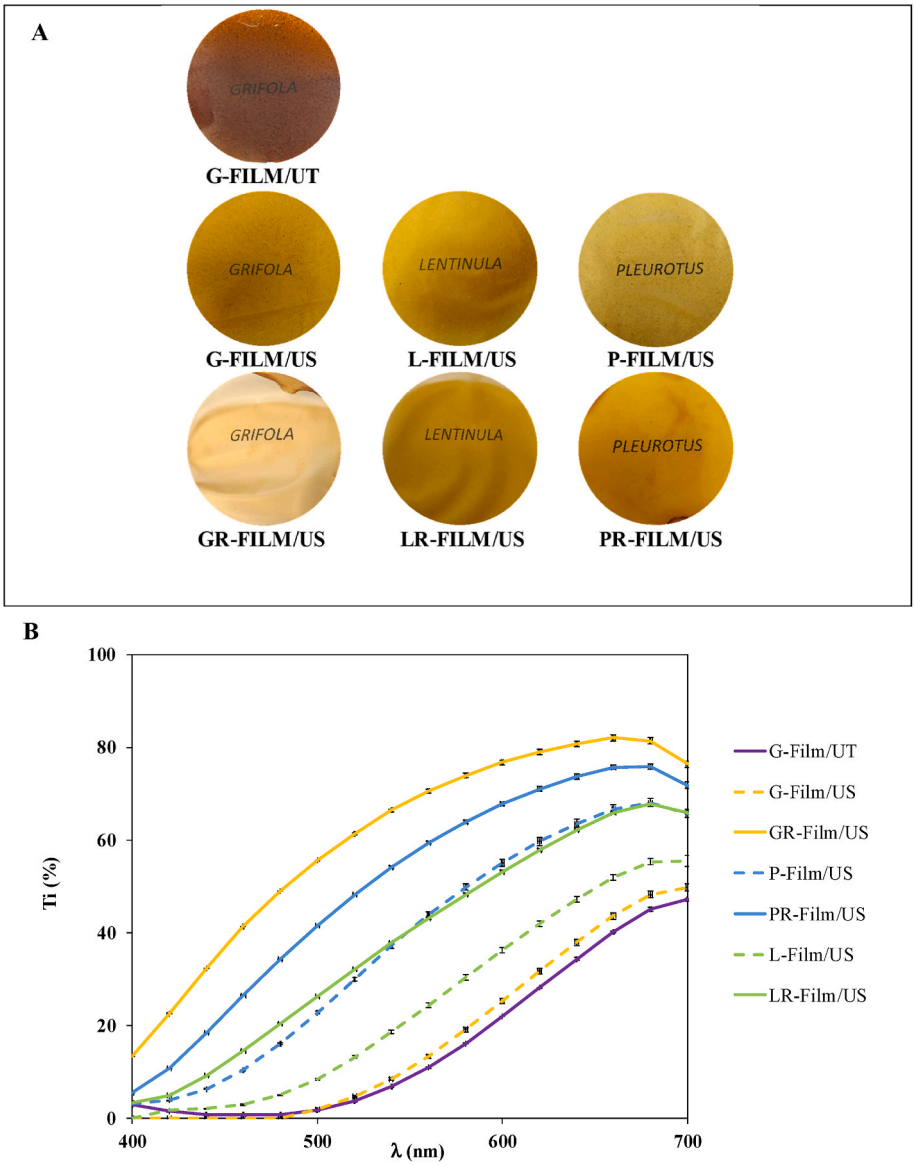

Fig. 3. **(A)** Visual appearance and **(B)** spectral distribution of internal transmittance (Ti) of the developed films using the whole mushrooms (G: *G. frondosa,* L: *L edodes* and P: *P. ostreatus*) or the residues from GR (*G. frondosa*), LR (*L edodes*) and PR (*P. ostreatus*) left after the aqueous and alkaline treatments. US and UT refer to ultrasound or UltraTurrax treatments, respectively, used for the production of fungal-based films.

that sonication improved the film forming capacity of those obtained from the mushrooms' discards, not being able to produce films when only UT treatment was used, except in the case of *G. frondosa*. Intense sonication conditions can cleave glycosidic bonds, disrupting polysaccharide interactions within the cell wall or reducing their molecular weight (Chen, Chen, Lin, Liu, & Cheung, 2015). This, in turn, allows the formation of a continuous film. In contrast, the dispersion of the samples by UT treatment, only enabled film formation in the samples where these components were already present, which in *G. frondosa* might be related to its higher recalcitrance and lower presence of water-soluble beta-glucans (Pérez-Bassart, Fabra, Martínez-Abad, & López-Rubio, 2023).

Furthermore, the residues generated after the extraction of β-glucans from the three different species by applying hot-water treatments followed by an alkali treatment were also valorised in this work to evaluate the possibility of forming films from aqueous suspensions using US. In this case, residues were already subjected to aqueous and alkaline treatments, removing specific components (salts, small peptides and oligosaccharides, polyphenols, pigments, and other secondary metabolites, proteins), which might hinder film formation. Therefore, films were formed from these residues by UT or US treatments for all tested species.

3.2.1. Optical properties and morphology

Fig. 3A shows the visual appearance of the produced films. All the films were translucent and presented a yellow-brownish tonality. It is well-known that the transparency of the films is directly linked with the internal structure of the developed films (Fabra et al., 2009). Thus, the effect of discarded mushroom composition and the residues was quantitatively assessed through the internal transmittance (Ti) measurements. As observed in Fig. 3B, Ti's spectral distribution curves depended on the matrices' internal microstructure and the composition and distribution of the films' components. The discarded mushroom biomass films presented much lower transmittance values than their counterparts prepared with the residues, making these films more opaque and heterogeneous. This effect could be attributed to the differences in refractive indices among films' components such as proteins, lipids and polyphenols (an increase in light scattering). Also, the selective light absorption of some compounds (i.e polyphenols) at low wavelengths was more accentuated in the case of *G. frondosa* films which had a higher polyphenol content (see Table 1).

SEM evaluated the produced films' morphology and representative images are shown in Fig. 4. Generally, a different internal arrangement was observed as a function of the raw material used and the homogenization conditions. *G. frondosa* discards films prepared with UT (Fig. 4A) showed a more heterogeneous cross-section and structural discontinuities suggesting a lack of miscibility of the components in this film. In contrast, films obtained from discarded biomass using the US treatment, showed a more continuous and softer microstructure than their counterparts prepared using UT, less compact than those obtained from the residue.

When the three species were compared, films obtained from *L. edodes* discards (Fig. 4D) exhibited the most homogeneous structure with no brittle areas or bubbles, consistent with forming a compact arrangement of biopolymer components (β-glucans and proteins). This is substantial evidence of differences in the cell wall architecture among the three species, which deserve further study.

A more compact and laminar-like structure was observed in the films obtained from the residues, which could be ascribed to the fibrillar structure of chitin embedded in the biopolymer matrix. The residual β-glucans and proteins remaining in the residue acted as a continuous amorphous matrix in which chitin fibrils were embedded. Fibrils from chitin were more clearly discerned in the *L. edodes* films (Fig. 4E) in agreement with its higher chitin content in the residue and the lower amount of β-glucans (see Fig. 1). Chitin fibres seem more embedded in the continuous β-glucan matrix in *G. frondosa* and *P. ostreatus* films produced from the residues (Fig. 4C and G).

As detailed below, these differences in the internal morphology of the films' cross-section could also explain the differences found in the mechanical and barrier properties.

3.2.2. ATR-FTIR and XRD analysis

To better understand the differences between the films obtained from the discarded biomass and the residues, they were characterized by

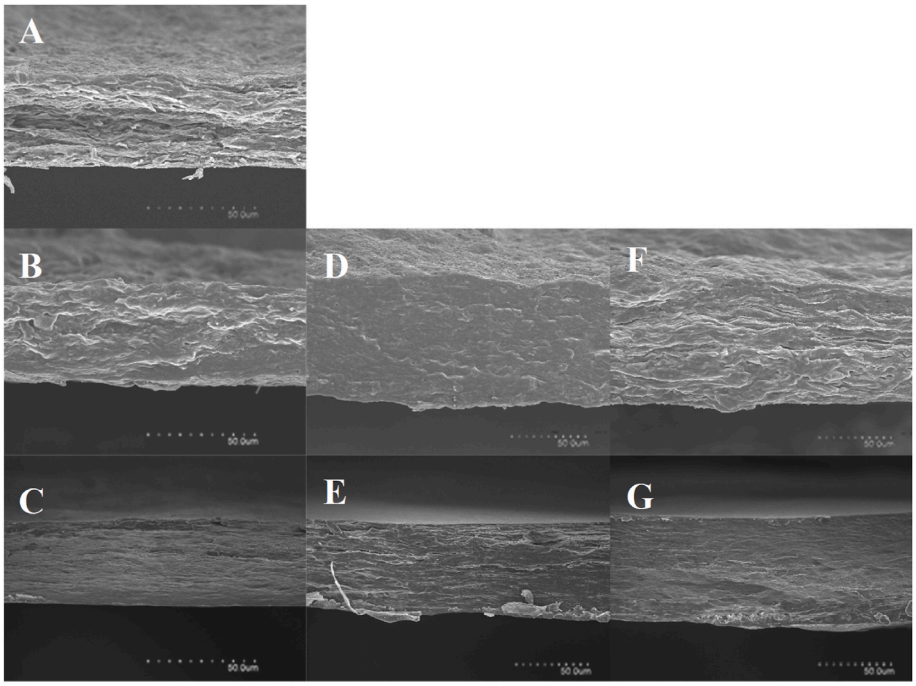

Fig. 4. SEM images of the cross-section from the developed films: **A** G-FILM/UT; **B** G-FILM/US; **C** GR-FILM/US; **D** L-FILM/US; **E** LR-FILM/US; **F** P-FILM/US; **G** PR-FILM/US.

FT-IR, and the obtained spectra are shown in Fig. 5. All samples generally showed broad bands at 3600-3200 cm^{-1} and 3000-2900 cm^{-1} attributed to O–H and C–H stretching, respectively, which presented very similar shapes. The broad band centered around 3300 cm^{-1} also contains contributions from the amide N–H stretching (3540-3125 cm^{-1}), which causes a sharpening of this band and further indicates the presence of higher amounts of proteins in the discarded biomass, in agreement with the proximal composition (see Table 1). Moreover, a sharper peak at 2924 cm^{-1} ascribed to vibrations of lipids was observed in the discarded mushrooms indicating the presence of small amounts of lipids in these samples, more accentuated in the case of *G. frondosa*. As expected, these peaks became less intense in the residues. This result evidences, in line with the proximal composition (see Table 1), that most proteins and lipids were removed during the aqueous and alkaline extraction processes and were in minor amounts in the residues.

Furthermore, several intense, highly overlapped IR bands in the regions 950-1200 cm^{-1}, mainly ascribed to C–C and C–O stretching vibrations in pyranoid rings, indicated the presence of polysaccharides as the main components. The presence of glucans in the discarded mushroom biomass and residues left after the aqueous and alkaline extractions was confirmed by the appearance of several characteristic bands located at 1100 and 1374 cm^{-1}. The weaker band located at 894 cm^{-1}, indicated the presence of β-glycosidic bonds in all the samples, mainly ascribed to β-glucans (Synytsya et al., 2009). This suggests that, as already anticipated, β-glucans remained in the residues obtained and were concentrated in the residue since other components have been proportionately removed after applying the aqueous and alkaline treatments. The peaks centered at 1650 cm^{-1} and 1540 cm^{-1} were assigned to amide I and amide II vibrations, respectively, of proteins and chitin.

To evaluate the impact of the mushroom's composition on the crystallinity of the films, the films were assessed by XRD analysis and the patterns are plotted in Fig. 6. All the patterns from the discarded biomass films showed several sharp and intense peaks arising from crystalline components such as minerals and salts, being more accentuated in the case of *L. edodes*. However, none of these peaks were visible in the spectra from the residue, suggesting that these components were removed upon the applied extraction processes.

In the case of the films obtained from the discarded biomass, all the samples were characterized by the appearance of a peak located at 19.3°, indicating the presence of crystalline GlcN (N-acetyl glucosamine) sequences from chitin, corresponding to the (110) crystal plane (Cárdenas, Cabrera, Taboada, & Miranda, 2004). As expected, the crystal structure changed notably in the films obtained from the residue. The relative intensity of this peak was significantly higher, except in the case of those obtained from *G. frondosa* residue, which almost disappeared after the aqueous and alkaline treatments. This effect may be related to the stronger chitin-glucan interactions and deserve further study. Interestingly, all the films obtained from the residue presented two prominent diffraction peaks located at 6.2° and 9.1°, which suggest a preferential orientation of (020) and (101) chitin crystal planes in the residues (Farinha et al., 2015). It is worth noting that the chitin peak at 9.1° has been associated with the most ordered regions involving the acetamide groups (Andrade et al., 2002) and also, with the randomly interplane layered structure (Wu, Mushi, & Berglund, 2020), shown in Fig. 3. A weak new diffraction peak was observed at 40° in films prepared from the *P. ostreatus* residue which may correspond to a second order peak of the previous intense diffraction peak centered at 20°. The diffraction peak at 40°, although more tenue, was also observed in films prepared from *L. edodes*.

The crystallinity of the films was estimated by fitting the areas under the diffraction patterns, resulting in values of *ca.* 25–27% for films prepared from discarded biomass and *ca.* 41, 30, and 29% for GR, LR and PR films, respectively. The resulting crystallinity degree can be ascribed to the presence of chitin in a crystalline form and other components from mushrooms that can be arranged during the film-forming process and they could contribute to the crystallinity degree. In fact, as deduced from Fig. 6, the peaks are wide suggesting that crystals were not perfectly defined and thus, not only chitin crystals but also other ordered components could contribute to the crystallinity.

3.2.3. Thermal properties of the films

DSC analysis was also carried out to study the thermal behaviour of the films. As shown in Fig. 7, a first endothermic peak was detected between 80 and 150 °C, ascribed to the bound water's evaporation (Kittur, Harish Prashanth, Udaya Sankar, & Tharanathan, 2002). On the other hand, a triple helix-single coil transition of (1,6) branched (1, 3)-β-glucans was previously reported in the same range (Kitamura et al., 1990; Liu, Wang, Cao, Xu, & Zhang, 2014). It is worth pointing out the main differences in this endothermic peak. While films from the residues left after the aqueous and alkaline treatment showed a sharper transition, the thermogram from films of discarded biomass showed a broader endothermic peak, which occurred at higher temperatures, indicating much more heterogeneous structures. According to previous reports, the triple helix of glucans can be dissociated to random coils when heated above 135 °C in aqueous solutions (Kitamura et al., 1990), evidenced by the higher temperatures at which the heat transition occurs in the films from discarded biomass. The sharp endothermic peak observed in the residues left after the aqueous and alkaline extractions can be mainly ascribed to the evaporation of water bound to the polysaccharides since the native structure of β-glucans were presumable lost during the harsh conditions used during the extraction protocol.

The exothermic event, including two exothermic decomposition peaks, evidences the presence of a mixture of chitin-glucan complexes usually associated with fungal cell walls (and detected during the compositional analysis), being more pronounced in the residues. Based on literature (Nováka et al., 2012; Pawlak & Mucha, 2003), the exothermic effect might result from cross-linking reaction between

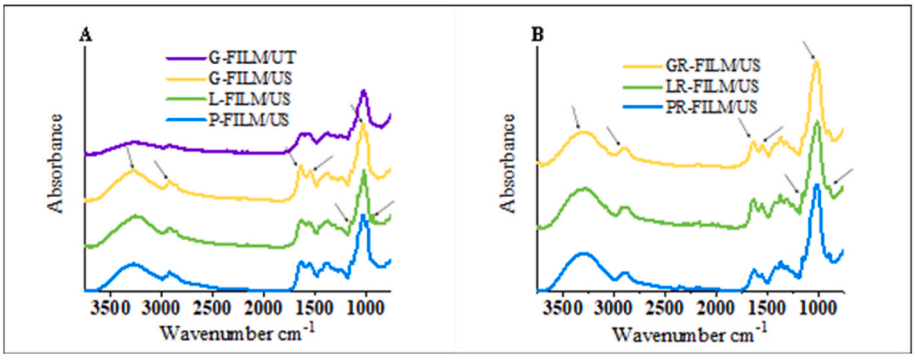

Fig. 5. FT-IR spectra of the developed films. Spectra have been offset for clarity. Arrows point out to the spectral bands displaying the most significant changes amongst the different samples.

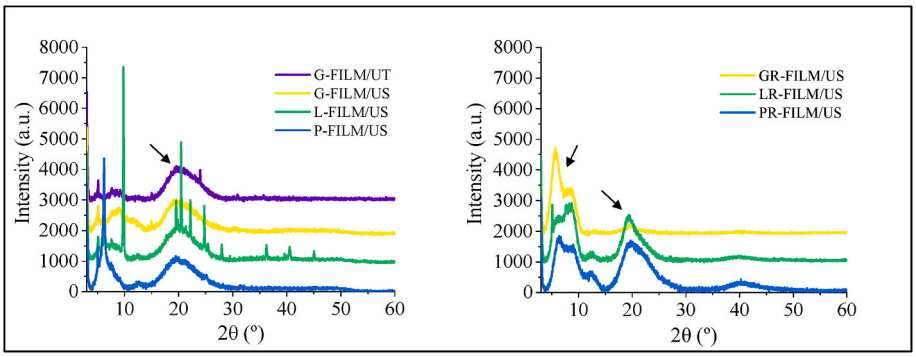

Fig. 6. XRD patterns of the films from (A) mushrooms' discards and (B) the residue.
The spectra from *G. frondosa* and *L. edodes* have been offset for clarity.

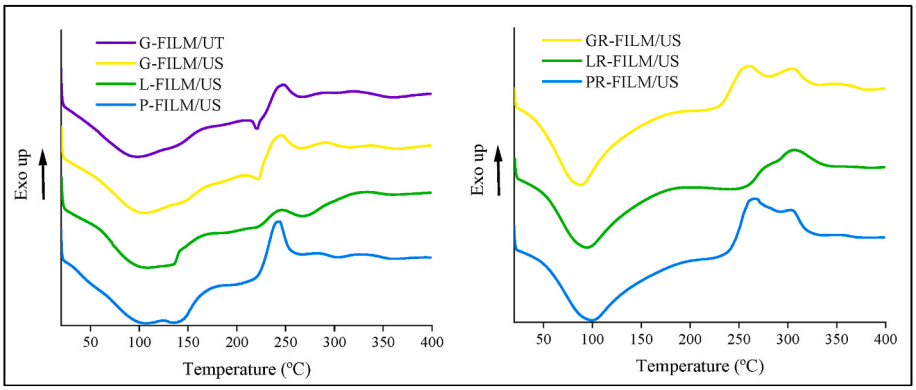

Fig. 7. DSC results of the obtained films.

polysaccharides (glucan and chitin), involving the destruction of free amino groups in chitosan generated during the alkali digestion. Differences in the residue composition and the recalcitrant nature of the β-glucans were also patent in the exothermic peaks. As clearly observed in Fig. 5b, the most recalcitrant *G. frondosa* residue showed two evident populations. Meanwhile, *L. edodes* showed a more intense peak at a higher temperature, probably related to chitin degradation (see Fig. 5) and ascribed to its higher chitin purity.

3.2.4. *Mechanical, barrier, water sorption and wettability properties of the films*

The tensile properties of the films are useful parameters to describe their mechanical behavior and are closely related to their internal structure. The most representative parameters from the stress-strain curves are summarized in Table 2. The mechanical properties of the films obtained from the discarded mushroom biomass were affected mainly by the species used and the homogenization conditions.

The first clear observation is that *L. edodes* films were more flexible, elastic, and deformable (presenting lower elastic modulus and tensile strength, and higher elongation at break) than the films from the other two mushrooms, in agreement with a more homogeneous distribution of mushroom' components in the film (see Fig. 3). This flexibility might be ascribed to higher hydrophilicity and plasticizing effect of the polysaccharide components. This could be related to a different structural organization of the β-glucans or/and to the higher abundance of mannogalactans, more hydrophilic than other heteropolysaccharides present in the other two species (Fig. S1). Furthermore, it has been demonstrated that a certain fraction of β-glucans present in the cell walls of *L. edodes* is bound to soluble proteins (Pérez-Bassart, Fabra, Martínez-Abad, & López-Rubio, 2023). Thus, it seems reasonable to hypothesize that the US treatment disrupts this interaction. A certain fraction of β-glucans and proteins are released into the aqueous medium, favoring the formation of a continuous matrix in which most of the components are well-integrated, interacting with the biopolymer matrix.

Table 2
Tensile properties (E: Elastic Modulus, TS: Tensile Strength and ϵ_b: Elongation at Break).

Film	E (MPa)	TS (MPa)	ϵ_b(%)
G-Film/UT	398 (34) ^{ab}	6.40 (0.19) ^{ab}	4.79 (0.59) ^{a}
G-Film/US	226 (50) ^{b}	4.64 (0.78) ^{ab}	3.00 (0.55) ^{ab}
GR-Film/US	3149 (46) ^{d}	33.59 (4.12) ^{c}	1.74 (0.43) ^{b}
L-Film/US	89 (15) ^{c}	3.63 (0.48) ^{a}	20.53 (2.71) ^{c}
LR-Film/US	4494 (180) ^{e}	28.68 (8.77) ^{c}	1.00 (0.18) ^{b}
P-Film/US	202 (25) ^{ac}	4.73 (0.82) ^{ab}	8.34 (2.67) ^{d}
PR-Film/US	2435 (196) ^{f}	11.08 (1.93) ^{b}	0.90 (0.14) ^{b}

E: Young's modulus; TS: tensile strength; ϵ_b: elongation at break; Values with different letters are significantly different ($p \leq 0.05$).

Regardless of the films obtained from the residues, all of them presented a very rigid behavior, with higher elastic modulus and lower elongation values, compared to their counterparts prepared with the mushrooms discards and ascribed to the higher crystallinity degree. The *L. edodes* residue provided less ductile films with higher TS values in agreement with the more fibrillar structure and its higher chitin content (see Figs. 1 and 3). In contrast, the residues from *P. ostreatus* gave rise to films that were more flexible and more ductile (lower E and TS values) than *G. frondosa*, an effect that can be explained by its lower crystalline degree and the type of crystals.

The films' oxygen and water vapor barrier properties were also measured, and the results are summarized in Table 3. Although there were no significant differences in the water vapor permeability of the films prepared with the three different species, *L. edodes* films were substantially less permeable. This is most likely due to the more compacted film structure, as evidenced by SEM. Similarly, this more

Table 3
Water vapor permeability (measured at 0–75% RH), water uptake (measured at 75% RH) and oxygen permeability values (measured at 50% RH) of the obtained films.

Film	WVP 10^{-14} ($Kg{\cdot}m{\cdot}Pa^{-1}{\cdot}\ s^{-1}{\cdot}m^{-2}$)	OP 10^{-19} ($m^3{\cdot}m{\cdot}Pa^{-1}{\cdot}s^{-1}{\cdot}m^{-2}$)	Water uptake (%)
G-Film/UT	18.58 (0.74) [a]	0.34 (0.17) [a]	23.9 (1.2) [a]
G-Film/US	9.44 (0.09) [b]	2.61 (0.47) [bc]	28.8 (2.3) [b]
GR-Film/US	18.73 (0.80) [a]	2.98 (0.18) [c]	17.2 (0.8) [cd]
L-Film/US	7.68 (0.29) [c]	0.91 (0.08) [d]	25.1 (2.8) [a]
LR-Film/US	19.88 (1.8) [a]	2.39 (0.12) [b]	15.8 (0.3) [d]
P-Film/US	8.36 (0.64) [bc]	1.25 (0.16) [d]	20.2 (0.7) [c]
PR-Film/US	22.37 (0.30) [d]	2.15 (0.12) [b]	13.6 (0.3) [d]
PLA[a]	13.1 (0.1)	17.8 (1.3)	0.95 (0.15)
Starch[b]	155.2 (1.0)	410 (23)	–

WVP: Water vapor permeability, OP: oxygen permeability. Values with different letters are significantly different ($p \leq 0.05$).
[a] Martínez-Sanz, Lopez-Rubio, & Lagaron, 2012
[b] Fabra, Martínez-Sanz, Gómez-Mascaraque, Gavara, & López-Rubio, 2018.

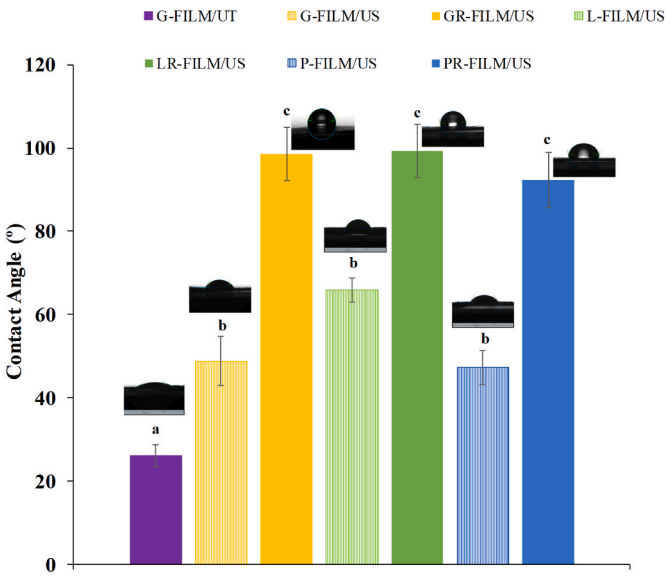

Fig. 8. Contact angle values and representative images of water droplets formed on the air-side of the developed films. Values followed by different letters are significantly different ($p \leq 0.05$).

homogenous and compact structure also resulted in better oxygen barrier properties than the films obtained with the other two mushroom species. After the aqueous and alkaline extractions, films obtained from the residues displayed lower barrier performance. Removing some lipids, proteins and polyphenol compounds from the residues could have negatively affected the barrier properties.

Compared to similar studies, in terms of barrier properties and production, the developed films in this study, outperformed benchmark biopolymers such as polylactic acid (PLA) (Martínez-Sanz et al., 2012) and starch (Fabra et al., 2018) with the additional advantages that they can be directly produced from fungal biomass.

As expected, the water sorption capacity of the films, measured through gravimetrical assays (see Table 3), was higher in films formulated with the whole mushroom biomass than their counterparts from the residues. This can be directly related to the more amorphous character of the matrices, thus being more accessible to moisture than the more crystalline fractions left after the extraction processes. In fact, the discarded biomass had a higher content on water soluble β-glucans, proteins, ashes and polyphenols which had a prominent hydrophilic nature which directly contributed to an increase in the water sorption. These results suggest that the lower permeability of the films prepared with the discarded mushroom biomass was partially related to the lower water diffusion because of the increased water sorption.

The water affinity of the films' surface was also evaluated through contact angle measurements which are normally used to estimate the degree of hydrophobicity of the material. The results are displayed in Fig. 8. The estimated contact angle of films prepared with the discarded mushroom biomass ranged between 23 and 65°. The mushroom residues yielded materials with much more hydrophobic surfaces after the extraction processes; may be due to the removal of hydrophilic compounds and amorphous compounds after the water and alkaline treatment, respectively, and also to a lesser amount of free hydroxyl groups in the surface of the films due to β-glucan-chitin interactions. Other biopolymeric films made of starch (Jiménez, Fabra, Talens, & Chiralt, 2012), PLA (Bonilla, Fortunati, Vargas, Chiralt, & Kenny, 2013), gelatin (George & Siddaramaiah, 2012) and PHB (polyhydroxybutyrate) (Pérez-Arauz et al., 2019; Urbina, Eceiza, Gabilondo, Corcuera, & Retegi, 2019) showed lower values than the ones obtained in the present work from the residues, demonstrating the high hydrophobicity of these materials and their potential applicability for food packaging (Urbina et al., 2019; Wang et al., 2020). Therefore, the residues promoted a more hydrophobic behavior at the surface of the films due to the absence of water-soluble molecules (including β-glucans). However, they had higher water vapor permeability values since the water molecules could quickly diffuse through the biopolymer network. In contrast, in the films obtained from the discarded biomass, thickness could increase during the WVP assays with the hydration shell of the biopolymer network and the subsequent decrease in mobility, impeding water diffusion, thus being a determining factor in the WVP. Therefore, the more amorphous character of the films obtained from discarded mushroom biomass may have promoted water sorption (higher values), producing greater swelling of the film matrix (lower contact angle) and, hence, yielding a structure that impedes water diffusion to a greater extent (lower WVP values).

A relevant aspect being highlighted is that, in contrast to the results observed for the discarded mushroom biomass, films from the residues could be generated by means of both UT and US. However, they did not show significant differences on the mechanical and barrier performance (see Supplementary Material S3).

3.3. Disintegration tests according to ISO 20200

One of the main advantages of biopolymers is that microorganisms can compost them within a certain time after use. The degree of disintegration is crucial to determine the bioplastics' compostability. In this work, the disintegration behavior of the developed films was compared and the results are shown in Fig. 9. In this process, the mass loss is considered as disintegrated material. Therefore, it calculates the degree of disintegration reached after the corresponding time.

Interestingly, significant differences were observed between films prepared from the discarded biomass and those obtained from the residue generated after the aqueous and alkaline extraction processes. As clearly observed in Fig. 9, although all of them were disintegrated before the end of the assay (90 days), thus indicating that the films were biodisintegrable, those prepared from the residue took more time than those prepared from the discarded biomass. This effect could be explained by the different compositions of the starting material and the physicochemical properties of the corresponding films. For instance, higher water uptake values (see Table 3) were obtained for films prepared from discarded biomass, being these ones more easily disintegrated than their counterparts obtained from the residues.

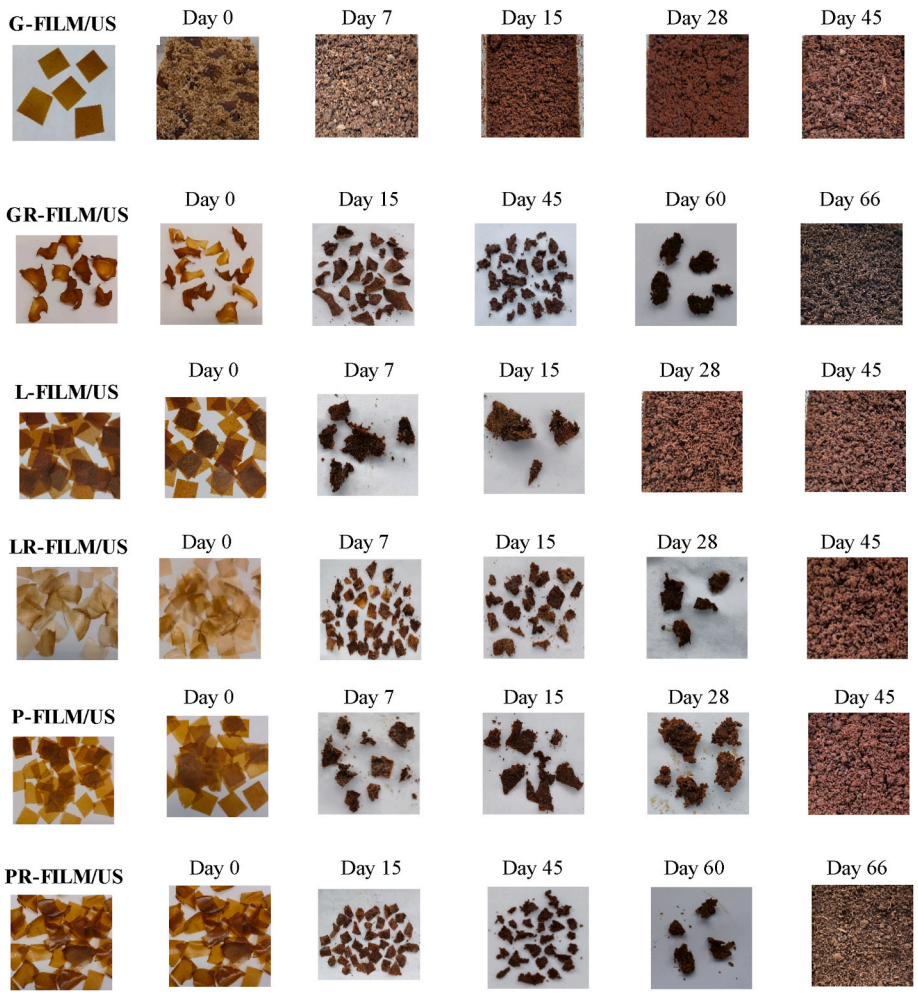

Fig. 9. Visual appearance of the samples before, during and after of the disintegration process.

Specifically, films prepared from *G. frondosa* discarded biomass were disintegrated entirely during the first week of the test. However, according to the standard, the test was maintained for a minimum of 45 days. In contrast, films generated from the residue obtained after the aqueous and alkaline treatments were more resistant than the film generated from the discarded biomass. In the first two weeks, the material absorbed water, doubling its thickness and giving it a gelly appearance. On day 45 of the test, the material's structure was soft and gradually disintegrated into smaller pieces. Total disintegration of the sample occurred on day 66.

In the case of films prepared from *L. edodes*, L-Film/US samples had an amber color, and they became darker and softer, and a quick fragmentation started during the first week of the disintegration assay. The mass loss was evident and the physical aspect corresponded to a wet paper. On day 15, very few sample pieces remained and it was wholly disintegrated after four weeks (28 days). Regarding the LR-Film/US samples, it was observed that they initially presented a light shade and became more opaque once the incubation period started. Similar to *G. frondosa* films, the disintegration time was the main difference concerning to films prepared from *L. edodes* discarded biomass; while the samples from the discarded mushroom disintegrated faster (28 days), the film from the residue took longer to reach a complete disintegration (45 days).

Similarly, films prepared from *P. ostreatus* discarded biomass (P-Film/US) disintegrated after 30 days of the assay. In contrast, those prepared from the residue (PR-Film/US) did not entirely degrade until day 66 of testing.

In general, the mass loss during the disintegration process until the films completely disappeared in the synthetic medium was an indicator that these materials could meet the compostability standard (EN13432) but, before affirming this, other tests corresponding to EN-13432:2001 should be carried out.

4. Conclusions

Fungal-based films were prepared from the discarded biomass of three different species (*Grifola frondosa, Lentinula edodes,* and *Pleurotus ostreatus*) and the corresponding residues were obtained after β-glucan extraction. The fungal biomass was mainly composed of carbohydrates, but significant amounts of proteins, lipids, and ashes were also detected. After the β-glucans extraction, polysaccharides were concentrated in the residue, mainly composed of chitin and residual β-glucans with some residual protein. Furthermore, the antioxidant activity and the phenolic compounds of the residues were significantly reduced compared to the mushrooms' discards. Chitin was more abundant in the *L. edodes* residue than in the other two residues and, although a significant amount of β-glucan remained in the residues, it was significantly higher for *G. frondosa* due to its greatest recalcitrance nature probably ascribed to stronger β-glucan-chitin bonds (as it did not have greater chitin content).

The discarded fungal biomass and the residues generated after β-glucan extraction were used to produce films (without plasticizers or other additives), which were characterized to evaluate their potential as food packaging materials. Overall, the films from the residue presented more desirable characteristics in terms of barrier, mechanical

properties, and visual appearance. Furthermore, according to the ISO 20200, all the films were disintegrable since they completely disappeared in a synthetic medium before 90 days of the assay.

Author statement

Z. Pérez-Bassart: Methodology, Investigation, Writing - original draft. **D. A. Martínez-Abad**: Methodology, Supervision, Writing - review & editing; **A. Reyes**: Methodology, Investigation **A. López-Rubio:** Conceptualization, Methodology, Funding acquisition, Project administration, Writing- Review. **M.J. Fabra:** Conceptualization, Methodology, Supervision, formal analysis, Funding acquisition, Project administration, Writing- Review.

Declaration of competing interest

The authors declare that there are no conflicts of interest.

Data availability

Data will be made available on request.

Acknowledgments

This research is part of the CSIC program for the Spanish Recovery, Transformation and Resilience Plan funded by the Recovery and Resilience Facility of the European Union, established by the Regulation (EU) 2020/2094. CSIC Interdisciplinary Thematic Platform (PTI+) Interdisciplinary Platform for Sustainable Plastics towards a Circular Economy+. (PTI-SusPlast+).

Appendix A. Supplementary data

Supplementary data to this article can be found online at https://doi.org/10.1016/j.foodhyd.2022.108174.

References

Aburas, H., İspirli, H., Taylan, O., Yilmaz, M. T., & Dertli, E. (2020). Structural and physicochemical characterisation and antioxidant activity of an α-D-glucan produced by sourdough isolate Weissella cibaria MED17. *International Journal of Biological Macromolecules, 161*, 648–655. https://doi.org/10.1016/J.IJBIOMAC.2020.06.030

Aguiló-Aguayo, I., Walton, J., Viñas, I., & Tiwari, B. K. (2017). Ultrasound assisted extraction of polysaccharides from mushroom by-products. *Lebensmittel-Wissenschaft & Technologie, 77*, 92–99. https://doi.org/10.1016/j.lwt.2016.11.043

Andrade, C. T., Silva, K. M. P., Tavares, M. I., Simão, R. A., Achete, C., & Pérez, C. A. (2002). Comparative study on structural features of α chitin from Xiphopenaeus kroyeri and its precipitated product from phosphoric acid solution. *Journal of Applied Polymer Science, 83*(1), 151–159. https://doi.org/10.1002/app.10017

ASTM. (2001). *ASTM Standard D 882 Standard test method for tensile properties of thin plastic sheeting*. ASTM Standards.

Bhargava, N., Sharanagat, V. S., Mor, R. S., & Kumar, K. (2020). Active and intelligent biodegradable packaging films using food and food waste-derived bioactive compounds: A review. In *Trends in food science and technology* (Vol. 105, pp. 385–401). Elsevier. https://doi.org/10.1016/j.tifs.2020.09.015.

Bonilla, J., Fortunati, E., Vargas, M., Chiralt, A., & Kenny, J. M. (2013). Effects of chitosan on the physicochemical and antimicrobial properties of PLA films. *Journal of Food Engineering, 119*(2), 236–243. https://doi.org/10.1016/j.jfoodeng.2013.05.026

Business Insights, F. (2019). *Market segmentation - mushroom market | fortune business Insights*. https://www.fortunebusinessinsights.com/industry-reports/segmentation/mushroom-market-100197.

Cárdenas, G., Cabrera, G., Taboada, E., & Miranda, S. P. (2004). Chitin characterization by SEM, FTIR, XRD, and13C cross polarization/mass angle spinning NMR. *Journal of Applied Polymer Science, 93*(4), 1876–1885. https://doi.org/10.1002/app.20647

Chen, J., Chen, L., Lin, S., Liu, C., & Cheung, P. C. K. (2015). Preparation and structural characterization of a partially depolymerized beta-glucan obtained from Poria cocos sclerotium by ultrasonic treatment. *Food Hydrocolloids, 46*, 1–9. https://doi.org/10.1016/J.FOODHYD.2014.12.005

Europe, P. (2021). *Plastics europe: Enabling a sustainable future. Plastics europe*. https://plasticseurope.org/.

Eyigor, A., Bahadori, F., Yenigun, V. B., & Eroglu, M. S. (2018). Beta-Glucan based temperature responsive hydrogels for 5-ASA delivery. *Carbohydrate Polymers, 201*, 454–463. https://doi.org/10.1016/j.carbpol.2018.08.053

Fabra, M. J., Martínez-Sanz, M., Gómez-Mascaraque, L. G., Gavara, R., & López-Rubio, A. (2018). Structural and physicochemical characterization of thermoplastic corn starch films containing microalgae. *Carbohydrate Polymers, 186*, 184–191. https://doi.org/10.1016/j.carbpol.2018.01.039

Fabra, M. J., Talens, P., & Chiralt, A. (2009). Microstructure and optical properties of sodium caseinate films containing oleic acid-beeswax mixtures. *Food Hydrocolloids, 23*(3), 676–683. https://doi.org/10.1016/j.foodhyd.2008.04.015

Farinha, I., Duarte, P., Pimentel, A., Plotnikova, E., Chagas, B., Mafra, L., et al. (2015). Chitin-glucan complex production by Komagataella pastoris: Downstream optimization and product characterization. *Carbohydrate Polymers, 130*, 455–464. https://doi.org/10.1016/j.carbpol.2015.05.034

George, A., Sanjay, M. R., Srisuk, R., Parameswaranpillai, J., & Siengchin, S. (2020). A comprehensive review on chemical properties and applications of biopolymers and their composites. In *International journal of biological macromolecules* (Vol. 154, pp. 329–338). Elsevier. https://doi.org/10.1016/j.ijbiomac.2020.03.120.

George, J., & Siddaramaiah. (2012). High performance edible nanocomposite films containing bacterial cellulose nanocrystals. *Carbohydrate Polymers, 87*(3), 2031–2037. https://doi.org/10.1016/j.carbpol.2011.10.019

Girometta, C., Dondi, D., Baiguera, R. M., Bracco, F., Branciforti, D. S., Buratti, S., et al. (2020). Characterization of mycelia from wood-decay species by TGA and IR spectroscopy. *Cellulose, 27*(11), 6133–6148. https://doi.org/10.1007/s10570-020-03208-4

Grimm, D., & Wösten, H. A. B. (2018). Mushroom cultivation in the circular economy. *Applied Microbiology and Biotechnology, 102*(18), 7795–7803. https://doi.org/10.1007/s00253-018-9226-8

Ifuku, S., Nomura, R., Morimoto, M., & Saimoto, H. (2011). Preparation of chitin nanofibers from mushrooms. *Materials, 4*(8), 1417–1425. https://doi.org/10.3390/ma4081417

Jiménez, A., Fabra, M. J., Talens, P., & Chiralt, A. (2012). Edible and biodegradable starch films: A review. In *Food and bioprocess technology* (Vol. 5, pp. 2058–2076). Springer. https://doi.org/10.1007/s11947-012-0835-4. Issue 6.

Kalač, P. (2009). Chemical composition and nutritional value of European species of wild growing mushrooms: A review. *Food Chemistry, 113*(Issue 1), 9–16. https://doi.org/10.1016/j.foodchem.2008.07.077

Kitamura, S., Ozasa, M., Tokioka, H., Hara, C., Ukai, S., & Kuge, T. (1990). A differential scanning calorimetric study of the conformat ional transitions of several kinds of (1→6) branched (1→3)-β-d-glucans in a mixture of water and dimethylsulfoxide. *Thermochimica Acta, 163*(C), 89–96. https://doi.org/10.1016/0040-6031(90)80382-9

Kittur, F. S., Harish Prashanth, K. V., Udaya Sankar, K., & Tharanathan, R. N. (2002). Characterization of chitin, chitosan and their carboxymethyl derivatives by differential scanning calorimetry. *Carbohydrate Polymers, 49*(2), 185–193. https://doi.org/10.1016/S0144-8617(01)00320-4

Liu, Q., Wang, C., Cao, Y., Xu, X., & Zhang, L. (2014). A novel gene carrier prepared from triple helical β-glucan and polydeoxyadenylic acid. *Journal of Materials Chemistry B, 2*(8), 933–944. https://doi.org/10.1039/c3tb21195a

Martínez-Sanz, M., Lopez-Rubio, A., & Lagaron, J. M. (2012). Optimization of the dispersion of unmodified bacterial cellulose nanowhiskers into polylactide via melt compounding to significantly enhance barrier and mechanical properties. *Biomacromolecules, 13*(11), 3887–3899. https://doi.org/10.1021/BM301430J/ASSET/IMAGES/BM301430J.SOCIAL.JPEG_V03

Muzzarelli, R. A. A., Boudrant, J., Meyer, D., Manno, N., Demarchis, M., & Paoletti, M. G. (2012). Current views on fungal chitin/chitosan, human chitinases, food preservation, glucans, pectins and inulin: A tribute to henri braconnot, precursor of the carbohydrate polymers science, on the chitin bicentennial. *Carbohydrate Polymers, 87*(Issue 2), 995–1012. https://doi.org/10.1016/j.carbpol.2011.09.063

Nováka, M., Synytsyaa, A., Gedeonb, O., Slepičkac, P., Procházkab, V., Synytsyad, A., et al. (2012). Yeast β(1-3),(1-6)-d-glucan films: Preparation and characterization of some structural and physical properties. *Carbohydrate Polymers, 87*(4), 2496–2504. https://doi.org/10.1016/j.carbpol.2011.11.031

Pawlak, A., & Mucha, M. (2003). Thermogravimetric and FTIR studies of chitosan blends. *Thermochimica Acta, 396*(1–2), 153–166. https://doi.org/10.1016/S0040-6031(02)00523-3

Payne, J., McKeown, P., & Jones, M. D. (2019). A circular economy approach to plastic waste. In *Polymer degradation and stability* (Vol. 165, pp. 170–181). Elsevier. https://doi.org/10.1016/j.polymdegradstab.2019.05.014.

Pérez-Arauz, A. O., Aguilar-Rabiela, A. E., Vargas-Torres, A., Rodríguez-Hernández, A. I., Chavarría-Hernández, N., Vergara-Porras, B., et al. (2019). Production and characterization of biodegradable films of a novel polyhydroxyalkanoate (PHA) synthesized from peanut oil. *Food Packaging and Shelf Life, 20*, Article 100297. https://doi.org/10.1016/j.fpsl.2019.01.001

Pérez-Bassart, Z., Fabra, M. J., Martínez-Abad, A., & López-Rubio, A. (2023). *Shedding some light on β-glucan extraction from three relevant mushrooms. 402*. Food Chemistry, Article 134207. doi.org/10.1016/j.foodchem.2022.134207.

Puanglek, S., Kimura, S., Enomoto-Rogers, Y., Kabe, T., Yoshida, M., Wada, M., et al. (2016). In vitro synthesis of linear α-1,3-glucan and chemical modification to ester derivatives exhibiting outstanding thermal properties. *Scientific Reports, 6*(1), 1–8. https://doi.org/10.1038/srep30479

Savadekar, N. R., & Mhaske, S. T. (2012). Synthesis of nano cellulose fibers and effect on thermoplastics starch based films. *Carbohydrate Polymers, 89*(1), 146–151. https://doi.org/10.1016/j.carbpol.2012.02.063

Synytsya, A., Míčková, K., Synytsya, A., Jablonský, I., Spěváček, J., Erban, V., et al. (2009). Glucans from fruit bodies of cultivated mushrooms Pleurotus ostreatus and

Pleurotus eryngii: Structure and potential prebiotic activity. *Carbohydrate Polymers, 76*(4), 548–556. https://doi.org/10.1016/j.carbpol.2008.11.021

Synytsya, A., & Novák, M. (2013). Structural diversity of fungal glucans. In *Carbohydrate polymers* (Vol. 92, pp. 792–809). Elsevier. https://doi.org/10.1016/j.carbpol.2012.09.077. Issue 1.

Urbina, L., Eceiza, A., Gabilondo, N., Corcuera, M.Á., & Retegi, A. (2019). Valorization of apple waste for active packaging: Multicomponent polyhydroxyalkanoate coated nanopapers with improved hydrophobicity and antioxidant capacity. *Food Packaging and Shelf Life, 21*, Article 100356. https://doi.org/10.1016/j.fpsl.2019.100356

Vetter, J. (2007). Chitin content of cultivated mushrooms Agaricus bisporus, Pleurotus ostreatus and Lentinula edodes. *Food Chemistry, 102*(1), 6–9. https://doi.org/10.1016/j.foodchem.2006.01.037

Wang, X., Huang, L., Zhang, C., Deng, Y., Xie, P., Liu, L., et al. (2020). Research advances in chemical modifications of starch for hydrophobicity and its applications: A review. In *Carbohydrate polymers* (Vol. 240)Elsevier, Article 116292. https://doi.org/10.1016/j.carbpol.2020.116292.

Wu, Q., Mushi, N. E., & Berglund, L. A. (2020). High-strength nanostructured films based on well-preserved α-chitin nanofibrils disintegrated from insect cuticles. *Biomacromolecules, 21*(2), 604–612. https://doi.org/10.1021/acs.biomac.9b01342

Zhu, F., Du, B., & Xu, B. (2016). A critical review on production and industrial applications of beta-glucans. *Food Hydrocolloids, 52*, 275–288. https://doi.org/10.1016/J.FOODHYD.2015.07.003